Control of Wave Energy Converters for Maximum Power Absorption with Time Domain Analysis

KARA, Fuat

Published version

KARA, Fuat (2017). Control of Wave Energy Converters for Maximum Power Absorption with Time Domain Analysis. Journal of Fundamentals of Renewable Energy and Applications, 07 (01).

Journal of Fundamentals of Renewable Energy and Applications

Kara, J Fundam Renewable Energy Appl 2017, 7:1
DOI: 10.4172/2090-4541.1000221

Review Article OMICS International

Control of Wave Energy Converters for Maximum Power Absorption with Time Domain Analysis

Fuat Kara*

School of Water, Energy and Environment, Cranfield University, UK

Abstract

A discrete control of latching is used to increase the bandwidth of the efficiency of the Wave Energy Converters (WEC) in regular and irregular seas. When latching control applied to WEC it increases the amplitude of the motion as well as absorbed power. It is assumed that the exciting force is known in the close future and that body is hold in position during the latching time. A heaving vertical-cylinder as a point-absorber WEC is used for the numerical prediction of the different parameters. The absorbed maximum power from the sea is achieved with a three-dimensional panel method using Neumann-Kelvin approximation in which the exact initial-boundary-value problem is linearized about a uniform flow, and recast as an integral equation using the transient free-surface Green function. The calculated response amplitude operator, absorbed power, relative capture width, and efficiency of vertical-cylinder compared with analytical results.

Keywords: Time domain; Transient free-surface green function; Boundary integral equation; Absorbed power; Relative capture width; Latching control

Introduction

The issue of global warming has resulted in growing pressure to switch to renewable sources (e.g. solar, wind, wave, tidal, geothermal, ocean thermal etc.) to reduce carbon emissions. Of these, ocean wave power has received much attention in Europe and other part of the world. The global power potential represented by waves that hit all coasts worldwide is estimated to be in the order of 1 TeraWatt (TW) [1]. If wave energy loss due to friction and wave breaking may be utilised, then the global wave power input is estimated to be one order of magnitude larger (≈10 TW), a quantity that is comparable with the world's present power consumption. The idea of converting the energy of ocean waves into useful energy forms is not new. There are techniques that were first patented as early as 1799 [2]. The pioneer work for the wave energy utilisation was introduced in the late 1940s by Masuda [3], Salter [4], Budal et al. [5], McCormick [6], Mei [7]. For an axisymmetrical WEC in regular waves, it is known that the maximum power that can be absorbed equals the incident wave power associated with a wave front of width one wave length divided by 2π. This result was first derived independently by Budal et al. [8], Evans [9] and Newman [10].

Power from ocean waves can be converted useful energy (e.g. electrical energy) by the use of Oscillating Water Columns (OWC) or OverTopping Devices (OTD) exploiting power of the seawater or oscillating devices (e.g. point absorber devices) in near shore or offshore environment exploiting body motion of the devices which excited by the incident waves [11]. OWC and OTD devices have large horizontal extension and large broad bandwidth whilst point absorber devices can take incident waves at any direction and have narrow bandwidth which allows the use of optimum control strategies (e.g. latching control) effectively. It is possible to convert wave energy to some other form; mechanical, hydraulic or pneumatic at very high efficiencies. The problem of converting this primary energy to a marketable product has presented the greatest challenge to various WEC inventors. The main reason for the very difficult engineering problems is the fact that waves transfer their energy in a slow irregular fashion whereas current technology, particularly for electrical generation, is more used to fast regular movements.

WEC without control traps energy only from the wave components whose frequency lies in the band of the natural frequencies of the system. Nevertheless, this system is potentially able to catch energy in the wave spectrum outside this band provided it can be dynamically controlled to adapt its bandwidth in real time. In this way, the power output from WEC can be increased by controlling the oscillation in order to approach an optimum interaction between WEC and incident wave. Optimum control methods can be classified for WEC as reactive (continuous) and latching (discrete) controls. Applying reactive control to WEC allows absorption of the maximum power [12]. In reactive control, the applied force/moments are a continuous function of time, and generally include resistive and reactive components to approach resonance at wave frequencies lower than the natural frequency of WEC. In latching control [11] while the motion is locked, the wave exciting force continues to evolve. Latching control involves braking and releasing the oscillating body such that its velocity bears the desired phase relationship with the wave-applied exciting force.

The damping of WEC must be properly adjusted in order to obtain approximate optimum amplitude. This is accomplished by Power-Take-Off (PTO) system. PTO mechanism is idealized by damping coefficients, giving forces proportional to the velocity of WEC. In the context of mathematical modelling, since the objective with WEC is to induce a movement such that radiated waves cancel in amplitude and phase with the scattered component to a maximum extend, the accurate predictions of radiated and diffracted waves due to forced oscillation of WEC and exciting forces, respectively are crucially important. This ensures that as little energy as possible is in the resultant outgoing wave field and therefore the maximum energy is observed by WEC. The accurate and computationally efficient numerical model was developed

***Corresponding author:** Fuat Kara, School of Water, Energy and Environment, Cranfield University, UK, Tel: 44 (0) 1234 754118; E-mail: f.kara@cranfield.ac.uk

Received December 09, 2016; **Accepted** January 12, 2017; **Published** January 16, 2017

Citation: Kara F (2017) Control of Wave Energy Converters for Maximum Power Absorption with Time Domain Analysis. J Fundam Renewable Energy Appl 7: 221. doi:10.4172/20904541.1000221

by the author [13,14] for the prediction of the hydrodynamics and power characteristics of WEC in regular waves. In the present paper, latching control for vertical-cylinder as a wave energy converter will be used to maximize the absorbed energy from both regular and irregular ocean waves. Equation of motion is considered in section 2 while solution of the integral equation is covered in section 3. Importance of latching control strategy in order to maximise the captured power is studied in section 4 whilst the main conclusions are given in section 5.

Equation of Motion of Wave Energy Converters

The right-handed coordinate system is used to define the fluid action. A Cartesian coordinate system $\vec{x} = (x, y, z)$ is fixed to the body. Positive *x*-direction is towards the bow, positive z-direction points upwards, and the z=0 plane (or *xy* plane) is coincident with calm water. The body is translating through an incident wave field with velocity U_0, while it undergoes oscillatory motion about its mean body surface position. The origin of the body-fixed coordinate system $\vec{x} = (x, y, z)$ is located at the centre of the *xy* plane. The solution domain consists of the fluid bounded by the free surface $S_f(t)$, the body surface $S_b(t)$, and the boundary surface at infinity S_∞ as in shown in Figure 1.

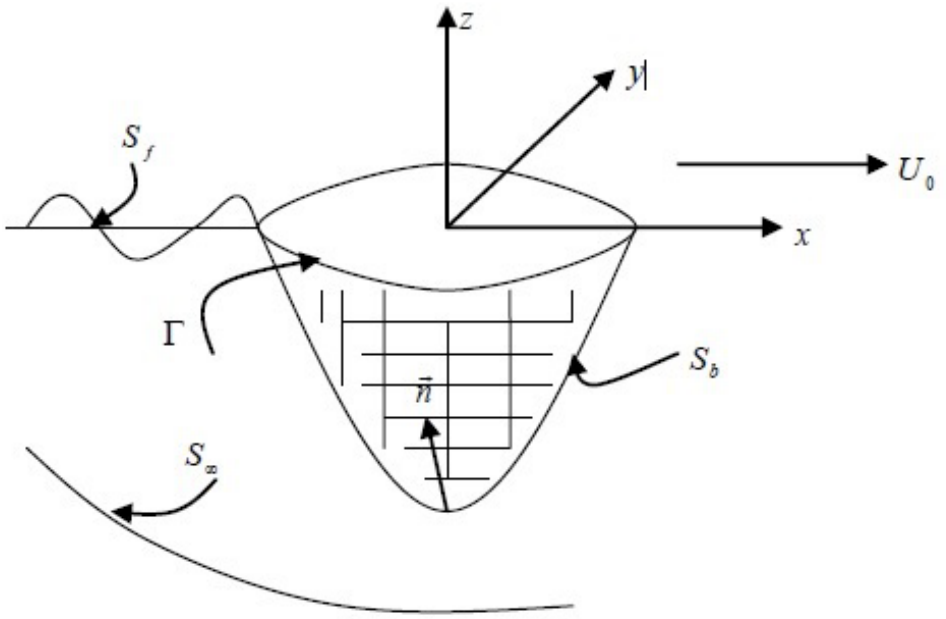

Figure 1: Coordinate system and surface of the problem.

Through Newton's law, the dynamics of a floating body's unsteady oscillations are governed by a balance between the inertia of the floating body and the external forces acting upon it. This balance is complicated by the existence of radiated waves; as a consequence both of the floating body's own motions and its scattering of the incident waves. This means that waves generated by the floating bodies at any given time will persist indefinitely and the waves of all frequencies will be generated on the free surface. These generated waves, in principle, affect the fluid pressure field and hence the body force of the floating bodies at all subsequent times. This situation introduces memory effects and is described mathematically by a convolution integral. Having assumed that the system is linear, the equation of motion of any floating rigid body may be written in a form which is essentially proposed by Cummins [15].

$$\sum_{k=1}^{6}(M_{jk}+a_{jk})\ddot{x}_k(t)+(B_{PTO}+b_{jk})\dot{x}(t)+(C_{jk}+c_{jk})x_k(t)+\int_0^t d\tau\, K_{jk}(t-\tau)\dot{x}(\tau)=\int_{-\infty}^{\infty} d\tau K_{jD}(t-\tau)\zeta(\tau) \quad (1)$$

$$j=1,2,\ldots,6$$

The displacement of the floating bodies from its mean position in each of its six rigid-body modes of motion is given x_k in Equation (1), and the overdots indicates differentiation with respect to time. The inertia matrix of the floating body is M_{jk}, damping due to PTO system is given as B_{PTO} and linearized hydrostatic restoring force coefficients are given by C_{jk}. The radiation impulse response functions are composed of the hydrodynamic coefficients and the kernel of the convolution on the left-hand side of Equation (1). A radiation impulse response function is the force on the body in the *j-th* direction due to an impulsive velocity in the *k-th* direction, with the coefficients a_{jk}, b_{jk}, c_{jk}, accounting for the instantaneous forces proportional to the acceleration, velocity, and displacement, respectively, and the memory function $K_{jk}(t)$ accounting for the free surface effects which persist after the motion occurs. For the radiation problem the term 'memory function' will be used to distinguish this portion of the impulse-response function from the instantaneous force components outside of the convolution on the left-hand side of Equation (1). The term $K_{jD}(t)$ on the right hand side of Equation (1) are the components of the exciting force and moment's impulse response functions due to the incident wave elevation $\zeta_0(t)$, defined at a prescribed reference point in the body-fixed coordinate system. Here, the kernel $K_{jD}(t)$ is the diffraction impulse response function; the force on the body in the *j-th* direction due to a uni-directional impulsive wave elevation with a heading angle of β. Once the stiffness

matrix, inertia matrix, and fluid forces e.g. radiation and diffraction forces are known, the equation of motion of floating body Equation (1) may be solved using the fourth order Runge-Kutta method.

Solution of Boundary Integral Equation

The initial boundary value problem consisting of initial condition, free surface and body boundary condition may be represented as an integral equation using a transient free surface Green's function [16]. Applying Green's theorem over the transient free surface Green function derives the integral equation. It is possible to show that transient free surface Green's function satisfies the initial boundary value problem without a body [17]. Integrating Green's theorem in terms of time from -∞ to ∞ using the properties of transient free surface Green's function and potential theory, the integral equation for the source strength on the body surface may be written as in Kara [18].

$$\sigma(P,t)+\frac{1}{2\pi}\iint_{S_b(t)} dS_Q \frac{\partial}{\partial n_P}\left(\frac{1}{r}-\frac{1}{r'}\right)\sigma(Q,t) = -2\frac{\partial}{\partial n_P}\varphi(P,t)-\frac{1}{2\pi}\int_{t_0}^{t} d\tau \iint_{S_b(\tau)} dS_Q \frac{\partial}{\partial n_P}\tilde{G}(P,Q,t-\tau)\sigma(Q,\tau)-\frac{U_0^2}{2\pi g}\int_{t_0}^{t} d\tau \oint_{\Gamma(\tau)} d\eta\, n_1 \frac{\partial}{\partial n_P}\tilde{G}(P,Q,t-\tau)\sigma(Q,\tau) \quad (2)$$

And potential on the body surface

$$\varphi(P,t) = -\frac{1}{4\pi}\iint_{S_b(t)} dS_Q \left(\frac{1}{r}-\frac{1}{r'}\right)\sigma(Q,t)-\frac{1}{4\pi}\int_{t_0}^{t} d\tau \iint_{S_b(\tau)} dS_Q\, \tilde{G}(P,Q,t-\tau)\sigma(Q,\tau)-\frac{U_0^2}{4\pi g}\int_{t_0}^{t} d\tau \oint_{\Gamma(\tau)} d\eta\, n_1\, \tilde{G}(P,Q,t-\tau)\sigma(Q,\tau) \quad (3$$

Where,

$\tilde{G}(P,Q,t,\tau)=2\int_0^\infty dk\sqrt{kg}\sin\left(\sqrt{kg}(t-\tau)\right)e^{k(z+\zeta)}J_0(kR)$ is the memory part of the transient free surface source potential, $P(x(t)\ y(t)\ z(t))$ the field point, $Q(\xi(t)\ \eta(t)\ \zeta(t))$ the source point, $r=\sqrt{(x-\xi)^2+(y-\eta)^2+(z-\zeta)^2}$ the distance between field and source point and represent the Rankine part of the source potential, $r'=\sqrt{(x-\xi)^2+(y-\eta)^2+(z+\zeta)^2}$ the distance between field point and image point over free surface, J_0 the Bessel function of zero order. The Green function $\tilde{G}(P,Q,t,\tau)$ represents the potential at the field point P (x, y, z) and time t due to an impulsive disturbance at source point $Q(\xi,\eta,\zeta)$ and time τ.

The integral equation for the source strength Equation (2) is first solved, and then this source strength is used in the potential formulation Equation (3) to find potential and velocities at any point in the fluid domain. The solution of the integral equation Equation (2) is done using time marching scheme. The form of the equation is consistent for both the radiation and the diffraction potentials so that the same approach may be used for all potentials. Since the transient free surface Green function $\tilde{G}(P,Q,t,\tau)$ satisfies free surface boundary condition and condition at infinity automatically, in this case only the underwater surface of the body needs to be discretized using quadrilateral/triangular elements. The resultant boundary integral equation Equation (2) is discretized using quadrilateral elements over which the value of the source strength is assumed to be constant and solved using the trapezoidal rule to integrate the memory or convolution part in time. This discretization reduces the continuous singularity distribution to a finite number of unknown source strengths. The integral equation Equation (2) has satisfied at collocation points located at the null points of each panel. This gives a system of algebraic equations which are solved for the unknown source strengths. At each time step the new value of the source strength is determined on each quadrilateral panel.

The evaluation of the Rankine source type terms (e.g. $1/r$, $1/r'$,) in Equation (2) is analytically integrated over quadrilateral panels using the method and formulas of Hess and Smith [19]. For small values of r the integrals are done exactly. For intermediate values of r a multi-pole expansion is used. For large values of r a simple monopole expansion is used.

The surface and line integrals over each quadrilateral element involving the wave term of the transient free surface Green function $\tilde{G}(P,Q,t,\tau)$ are solved analytically [20-22] and then integrated numerically using a coordinate mapping onto a standard region and Gaussian quadrature. For surface elements the arbitrary quadrilateral element is first mapped into a unit square. A two-dimensional Gaussian quadrature formula of any desired order is then used to numerically evaluate the integral. The line integral is evaluated by subdividing $\Gamma(t)$ into a series of straight line segments. The source strength $\sigma(t)$ on a line segment is assumed equal to the source strength of the panel below it.

The evaluation of the memory part $\tilde{G}(P,Q,t,\tau)$ of the transient free surface Green function and its derivatives with an efficient and accurate method is one the most important elements in this problem. Depending on the values of P, Q and t five different methods are used to evaluate $\tilde{G}(P,Q,t,\tau)$; power series expansion, an asymptotic expansion, a Filon integration quadrature, Bessell function, and asymptotic expansion of complex error function. Figure 2 shows the memory part $\tilde{G}(P,Q,t,\tau)$ of transient free surface Green function. The detail analysis of radiation and diffraction problem including Froude-Krylov force as well as numerical results that compared with analytical, experimental and other published numerical results can be found in Kara [13,14].

Latching Control of Offshore Wave Energy Converters

Latching control, which is a discrete real time control, will be used in the present paper. Rather than adapting WEC parameters to the excitation force in order to optimize the linear body response, the latching control adapts the body response to WEC and to the excitation in a nonlinear fashion. It is a kind of parametric resonance adaptation process as can be found in nonlinear oscillatory theory, this kind of behaviour can be predicted only using time domain simulations. Latching control can magnify the amplitude of the motion whatever the frequency of the excitation force, and can improve the efficiency of WEC in terms of absorbed energy for excitation frequencies. When latching control is applied, an additional force must be introduced in the dynamic of WEC to cancel the acceleration of the controlled motion in order to lock the system temporarily. The latching control of WEC consists of locking the oscillating body in position at the instant when velocity vanishes, and releasing it after a certain delay to be determined. This latching delay has to be applied in order to maximise the response amplitude of the body. The instant of latching is imposed by the dynamics of the body itself (i.e., vanishing velocity); thus the control variable is simply the duration of the latching phase, or equivalently the instant of release [23-27]. One of the advantages of latching control is that it is passive, which means that it does not need to deliver energy to WEC

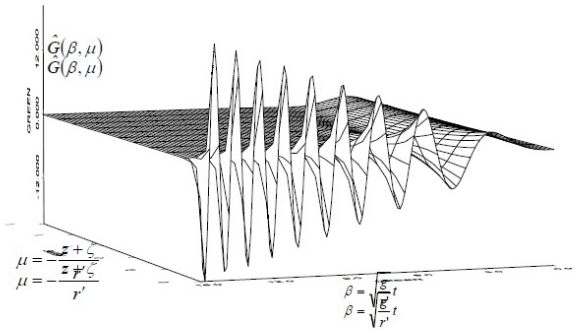

Figure 2: The memory part of the transient free surface Green function $\hat{G}(\beta,\mu)$.

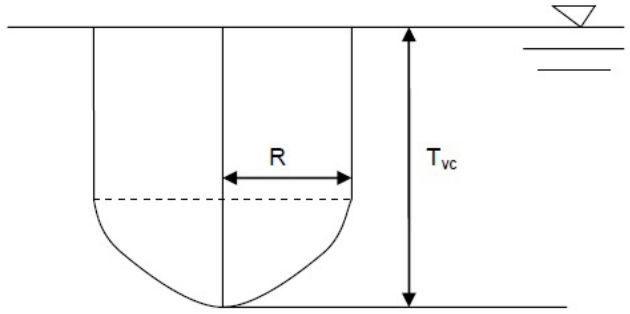

Figure 3: Geometry of vertical-cylinder.

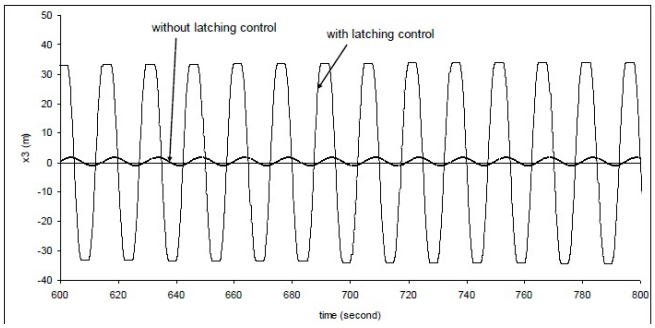

Figure 4: Heave motion amplitude of a vertical-cylinder wave energy converter with and without latching control at resonance period of 10 s and incident wave period at 15 s with 1 m wave amplitude.

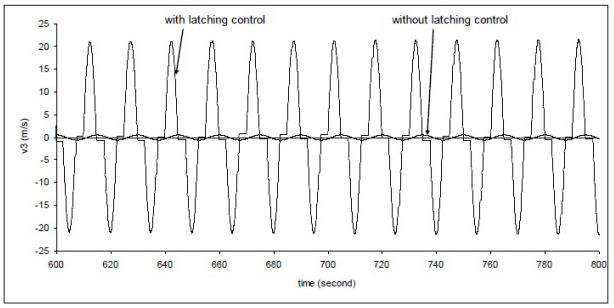

Figure 5: Heave velocity of a vertical-cylinder wave energy converter with and without latching control at resonance period of 10 s and incident wave period at 15 s with 1 m wave amplitude.

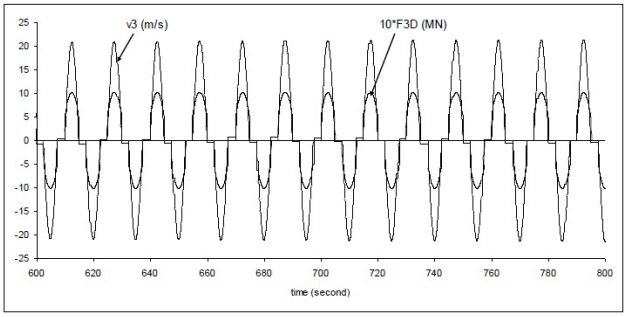

Figure 6: Heave velocity of a vertical-cylinder wave energy converter at resonance period of 10 s and exciting force at incident wave period of 15 s with 5 s latching control and 1 m wave amplitude.

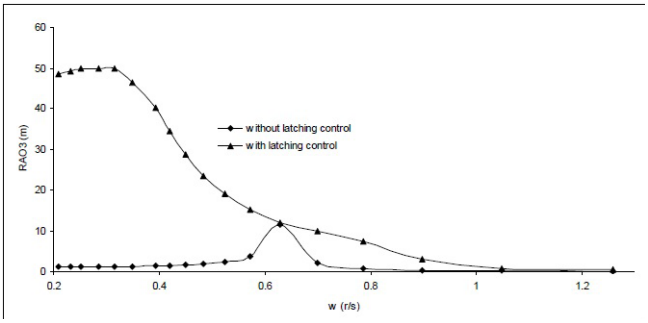

Figure 7: Heave response amplitude operator (RAO) with and without latching control for a vertical-cylinder with 10 s natural period and 1 m wave amplitude for different range of frequencies.

while it is engaged, since the forces do no work as long as the velocity vanishes.

Numerical results for regular waves

A vertical-cylinder with 8 m radius R and 13 m draft T_{vc} is used as an offshore floating wave energy converter in the following numerical results. The natural period T_n of the wave energy converter is 10 s. Geometry of vertical-cylinder is given in Figure 3.

Motion of wave energy converters with and without latching control: Budal and Falnes [11] point out that maximizing the extracted power requires that the wave force and the velocity of the wave energy converters be in phase. This condition is achieved when the velocity is vanishing. This implies that the wave energy converter is at its maximum displacement. The wave energy converter is hold until a prescribed time before the exciting force reaches its next extreme. This prescribed time is called the latching time which is a control variable. Our ITU-WAVE time domain program takes into account this latching strategy for a change in sign of the velocity which starts the latching.

In Figure 4, the numerical simulation in the time domain of the body response with and without latching control is plotted. The huge magnification of the amplitude of the motion for the controlled system compared to the uncontrolled one is observed. The amplitude of the

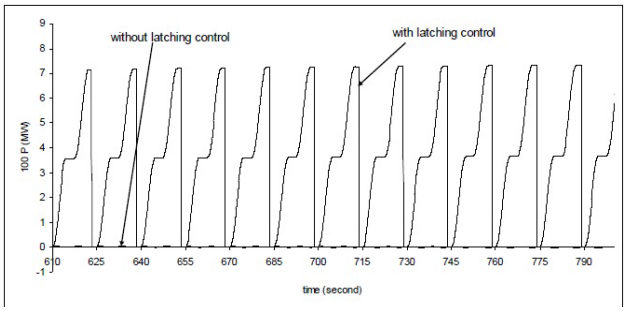

Figure 8: Instantaneous power absorbed by a vertical-cylinder at each period with and without latching control at resonance period of device at 10 s and incident wave period at 15 s with 1 m wave amplitude.

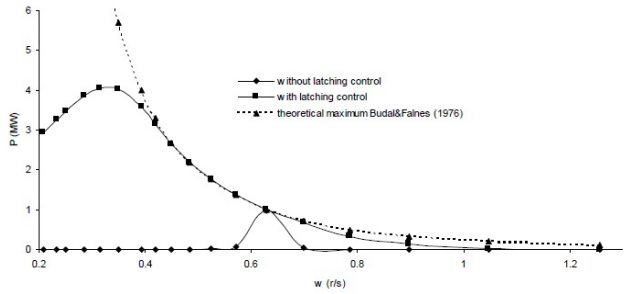

Figure 9: Absorbed mean power for a vertical-cylinder with and without latching control in the range of frequencies with 1 m wave amplitude.

heave motion is increased more than by a factor of 20 in the case of latching control.

Figure 5 shows velocity of wave energy converter with 5 s latching and without latching control. The device has 10 s resonance frequency and incident wave period is 15 s. One can observe a large amplification of the velocity of the device when latching control is applied as in motion amplitude of the heaving vertical-cylinder in Figure 4.

It is pointed out earlier that maximizing the extracted power requires that the wave force and the velocity of the wave energy converters be in phase when latching control is applied as shown in Figure 6. Latching duration can be observed from Figure 6.

It is assumed that the excitation force is known in the future of the current computation time. The motion of a wave energy converter under latching control is a succession of the time of the rest and time of the transient. The control variable is the release (or unlatching) time or equivalently the latching duration. We pointed out earlier that the aim of the latching control is to maximize the amplitude of the oscillations of the device. This implicitly means that it will also maximize the absorbed power at the same time. Figure 7 shows an example of numerical simulation of the body motion in a different incident wave period with and without latching control. It can be seen that the amplifying effect of latching control is significant in Figure 7. It may be noticed from Figure 7 that the response amplitude can be as much as by a factor of 50 in the case of latching control in higher incident wave periods.

Instantaneous and mean absorbed power: A damping force proportional to the velocity of the floating body is considered as the action of the external Power-Take-Off (PTO) mechanism. The

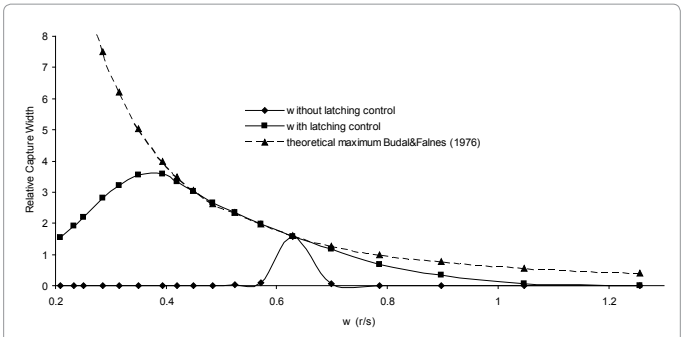

Figure 10: Relative capture width with and without latching control for a vertical-cylinder wave energy converter in the range of frequencies with 1 m wave amplitude.

instantaneous power converted by the wave energy converters is defined as:

$$P_{ins}(t) = P_e - P_r \tag{4}$$

Where, P_e is the power due to exciting force and P_r is the power due to radiation force.

Figure 8 shows the instantaneous power absorbed for each incident wave period of 15s from ocean waves using a vertical-cylinder as a wave energy converter with and without latching control. In the case of latching control the absorbed instantaneous power is increased significantly. It may be noticed that the unlatching results are very small in terms of controlled latching results.

The mean power $\overline{P}$ extracted by the PTO over a time range T is given by,

$$\overline{P}(t) = \overline{P}_e - \overline{P}_r \tag{5}$$

The averaging time T must be much larger than the characteristics period of the wave, which is typically 5 s to 15 s. The maximum mean power that can be absorbed is equal to the linear damping proportional to velocity of the floating body. This is achieved when the velocity is in phase with the exciting force [11] as it is shown in Figure 6.

Figure 9 shows the absorbed mean power for the range of incident wave frequencies using a vertical-cylinder as a wave energy converter with and without latching control. In the case of latching control the absorbed mean power is again increased significantly. The theoretical maximum power absorption in regular seas is given by Budal and Falnes [11].

$$P = \frac{\rho g^3 \zeta_0}{4\omega^3} \tag{6}$$

Where, ζ_0 being the incident wave amplitude and ω being incident wave frequency.

Capture width and relative capture width: The capture width l and maximum capture width l_{max} is defined as [11]:

$$l = \frac{\overline{P}}{P_w},\ l_{\max} = \frac{\lambda}{2\pi} \tag{7}$$

Respectively where $\overline{P}(t)$ is the mean power and given by Equation (5), $P_w = \rho g^2 \zeta_a^2 / 4\omega$ is the wave power in the incident wavetrain per unit crest length, ζ_a being the incident wave amplitude. A good wave absorber is a body which has the ability when making waves, to concentrate the wave energy along a narrow sector rather than distribute

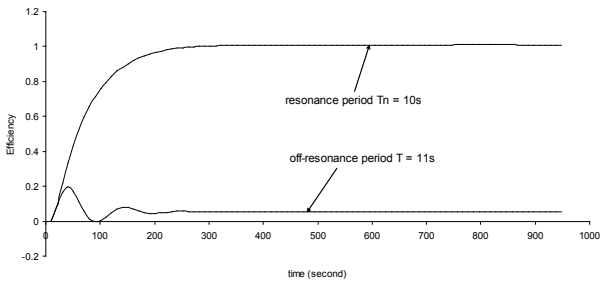

Figure 11: Convergence of efficiency for resonance and off-resonance period without latching control for a vertical-cylinder.

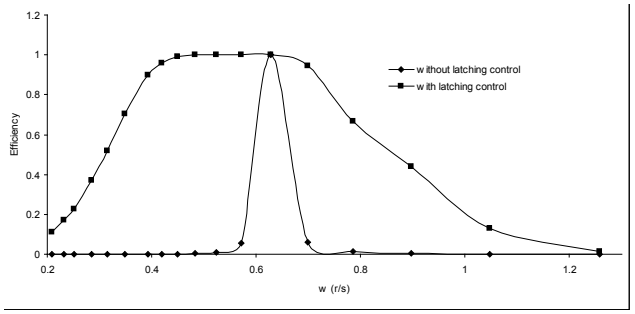

Figure 12: Efficiency with and without latching control for a vertical-cylinder wave energy converter in the range of frequencies.

the energy evenly over all angles. The maximum capture width equals to $\lambda/(2\pi)$ for an axisymmetric system in symmetric mode of motion e.g. heave. This implies that the floating body absorbs all the power in an incident wave equal to that passing a crest length of $\lambda/(2\pi)$. Relative capture width is obtained by dividing capture width with width B of the wave energy converters, $l_{rcw} = l/B$.

Figure 10 shows the relative capture width for with and without latching controlled system and the theoretical maximum in the context of linear theory are plotted. For such a single axisymmetric system in symmetric mode of motion e.g. heave the maximum capture width as pointed out earlier equals to $\lambda/(2\Pi)$. It may be noticed that it means that for low frequency waves, the absorbed power can possibly be greater than the incident power in the width of the body, implying capture widths greater than 1 and this can be observed in Figure 10. It can be also observed that latching control allows an improvement of the relative capture width whatever the frequency of the incident waves are.

Efficiency: The efficiency η of wave energy converters is defined as $\eta=l/l_{max}$, which has a maximum of 1.0 for any wavelength.

Figure 11 shows the efficiencies for vertical-cylinder in the case of in resonance and off-resonance periods. The efficiency converges to 1.0 (100% efficient) at resonance period T_n=10 s whereas off-resonance case T=11 s shows a very low efficiency (5%).

Figure 12 shows the efficiency plotted against the circular frequency for a vertical-cylinder which has 10 s (0.628 rad/s) natural period. If the natural period of vertical-cylinder equals the period of incident waves in the case of without latching control, the device is perfectly tuned and we expect optimal efficiency. As the difference between natural period of device and incident wave period increases, the efficiency of the system decreases. As can be seen in Figure 12 latching control increases the bandwidth of the wave energy converter for all frequency

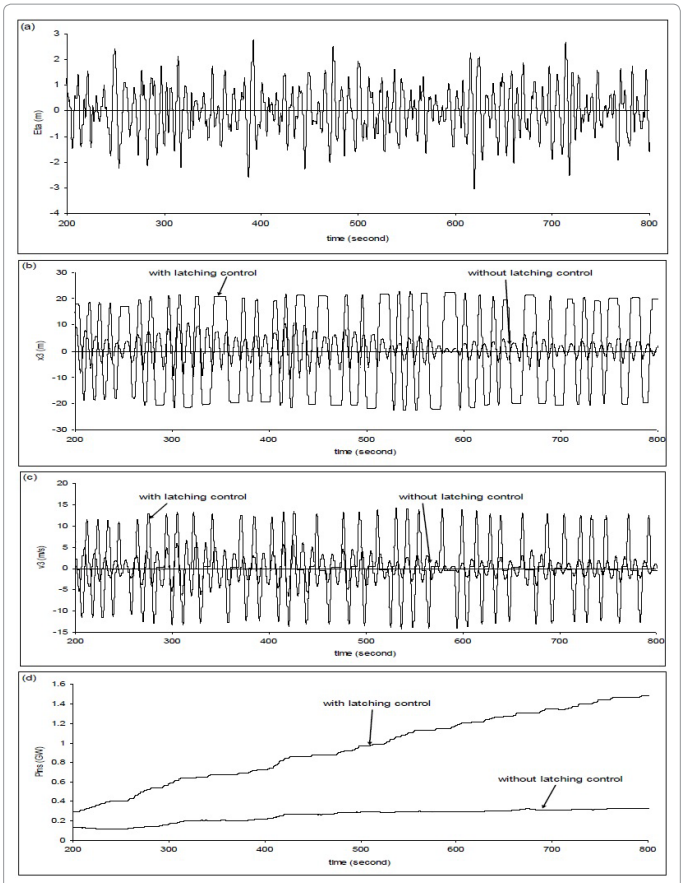

Figure 13: Comparison of different variables with and without latching control at natural period Tn=10 s and peak period Tp=10 s of vertical-cylinder wave energy converter (a) incident wave elevation at the origin of the wave energy converter (b) heave motion amplitude (c) heave velocity (d) accumulation of instantaneous power.

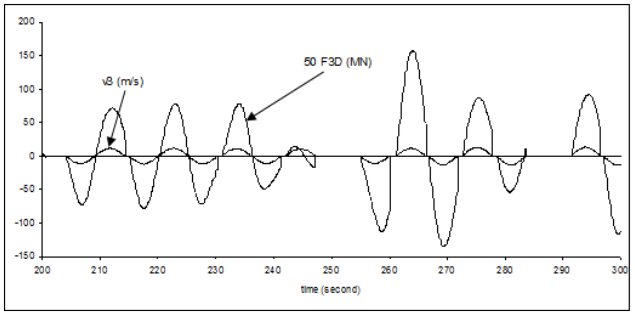

Figure 14: The velocity and exciting force of heaving vertical-cylinder at natural period Tn=10 s and peak period Tp=10 s.

ranges. If off-resonance period is 11s (0.571 rad/s), the efficiency is approximately 5% without latching control. However, if 1s latching is applied to vertical-cylinder wave energy converter, it is possible to achieve an efficiency of approximately 100%.

Numerical results for irregular waves

The Pierson-Moskowitz spectral formulation [28] developed from analysis of measured data obtained in the North Atlantic by wave recorders installed on weather ships will be used for irregular

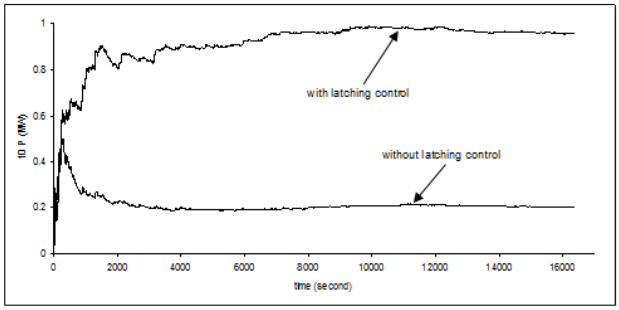

Figure 15: Convergence of mean power with and without latching control at natural period Tn=10 s and peak period Tp=10 s of vertical-cylinder wave energy converter.

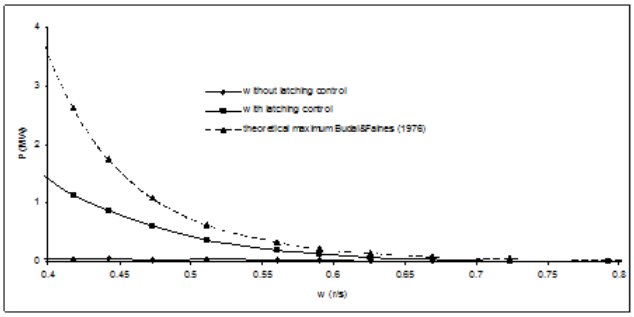

Figure 16: Absorbed mean power for a vertical-cylinder with and without latching control in the range of peak frequencies.

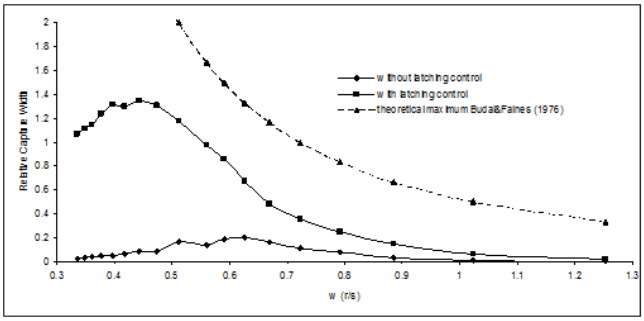

Figure 17: Relative capture width with and without latching control for a vertical-cylinder wave energy converter in the range of peak frequencies.

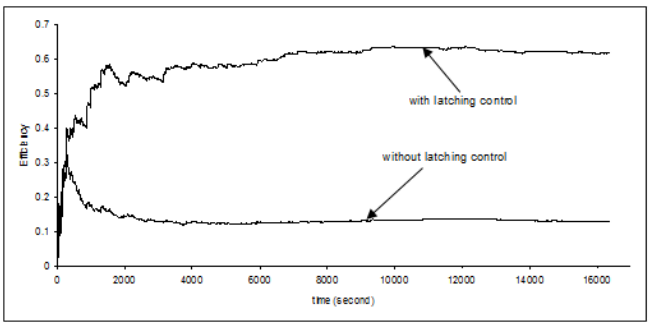

Figure 18: Convergence of the efficiency at natural period Tn=10 s and peak period Tp=10 s of vertical-cylinder wave energy converter.

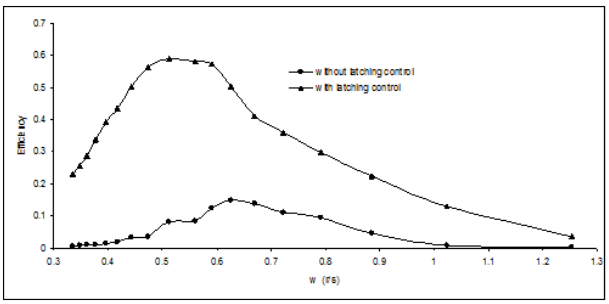

Figure 19: Efficiency with and without latching control for a vertical-cylinder wave energy converter in the range of peak frequencies.

seas. Analysis for this spectrum was carried out only on selected wave records considered to have been acquired in fully developed sea. The Pierson-Moskowitz spectrum can be presented in terms of significant wave height H_S. That is,

$$S(\omega)=\frac{8.10}{10^3}\frac{g^2}{\omega^5}\exp(-0.032\times(\frac{g}{H_s})^2/\omega^4) \quad (8)$$

The Pierson-Moskowitz spectral formulation depends on a single parameter, significant wave height, H_s. The relationship between significant wave height H_s and peak frequency ω_p is given as $\omega_p=0.4\times\sqrt{g/H_S}$ [29]. The theoretical maximum power absorption P in irregular seas is similar to the regular wave prediction and is given by Budal and Falnes [11].

$$P=\frac{\rho g^3(H_S(2\sqrt{2})}{4\omega_p^3} \quad (9)$$

The benefit of the latching control depends on the spectral characteristics of the incident wave. A wave energy converter will work with wave environment in which peak period ω_p is in the range of between 5 s and 15 s. The control variable that the body velocity vanishes remains invariant as in regular waves as well as the moment of unlatching in random sea environment.

Figure 13 shows the incident wave height which is the input for the numerical calculation of the exciting forces of diffraction and Froude-Krylov forces, heave displacement and velocity of the wave energy converter which is the response of the floating structure in the case of with and without latching control, and accumulated instantaneous absorbed power from the ocean.

Figure 14 shows the velocity and exciting force in phase in irregular wave case. The same strategy as in regular sea is used e.g. vanishing velocity that starts latching duration.

Figure 15 shows the convergence of the mean power. Prediction of the mean power for regular and irregular seas is done differently. In the case of regular seas, mean power is calculated for each incident period (Figure 8), while the accumulation of the instantaneous power is used for the irregular seas. It may be noticed in Figure 15 convergence of mean power requires more time in the case of irregular seas.

Figure 16 shows the absorbed mean power for the range of peak frequencies using a vertical-cylinder as a wave energy converter with and without latching control. In the case of latching control the absorbed mean power is again increased significantly.

Results are plotted in terms of relative capture width in Figure 17 as

a function of the peak frequencies. For each result the relative capture width of the same device without latching control is represented for the purpose of comparisons. As it is compared to the regular seas, the relative capture width is reduced almost 37% and occurs in higher peak frequencies.

Figure 18 shows convergence of the efficiency of wave energy converters in time at around peak frequency of 10s with and without latching control. As compared to regular seas, the convergence of efficiency needs more time. One of the reasons for this is that the accumulation of instantaneous power is used for the irregular seas rather than calculation of instantaneous power for each period.

Figure 19 shows the efficiency of vertical-cylinder with and without latching control. The general trend shows that latching control improves considerably the efficiency of the wave energy converters especially as the peak frequency of the wave environment increases. The maximum efficiency in irregular seas is around 60% as it is compared to 100% in regular seas.

Conclusion

A latching control with a transient hydrodynamic code for wave energy converters are used for the prediction of maximum power absorption from ocean waves for a point absorber heaving vertical-cylinder. Results have been presented to demonstrate the convergence of the method for power prediction of the floating wave energy converter and the calculation are shown to be in satisfactory agreement with analytical results. Results show that the efficiency of wave energy converters is considerably improved by the latching control which enlarges the bandwidth of WEC especially in the low frequencies, if the exciting force is predicted in the close future of the unlatching time.

References

1. Panicker NN (1976) Power resource potential of ocean surface waves. Proceedings of the wave and salinity gradient workshop, UAS.
2. Girard (1799) French Patent (translated by AE Hidden). Queens University, Belfast, UK.
3. Masuda Y (1986) An experience of wave power generator through tests and improvements. Hydrodynamics of Ocean Wave Energy Utilization. pp: 445-452.
4. Salter SH (1974) Wave power. Nature 249: 720-724.
5. Budal K, Falnes J (1974) Proposals for conversion of the energy in ocean waves. Internal Report, Norwegian University of Science and Technology.
6. McCormick M (1974) Analysis of a wave-energy conversion buoy. J Hydronautics 8: 77- 82.
7. Mei CC (1976) Power extraction from water waves. J Ship Res 20: 63-66.
8. Budal K, Falnes J (1975) A resonant wave point absorber of ocean waves. Nature 256: 478-479.
9. Evans D (1976) A theory for wave-power absorption by oscillating bodies. J Fluid Mech 77: 1-25.
10. Newman JN (1976) The interaction of stationary vessels with regular waves. Proceedings of the Eleventh Symposium on Naval Hydrodynamics. pp: 491-501.
11. Budal K, Falnes J (1976) Optimum operation of wave power converter. Internal Report, Norwegian University of Science and Technology.
12. Salter SH, Jeffery DC, Taylor JRM (1976) The architecture of nodding duck wave power generators. The Naval Architect. pp: 21-24.
13. Kara F (2010) Time domain prediction of power absorption from ocean waves with latching control. Renew Energy 35: 423-434.
14. Kara F (2016) Time domain prediction of power absorption from ocean waves with wave energy converters arrays. Renew Energy 92: 30-46.
15. Cummins WE (1962) The impulse response function and ship motions. Shiffstechnik 9: 101-109.
16. Wehausen JV, Laitone EV (1960) Surface waves. Handbuch der Physik 9: 446-778.
17. Finkelstein AB (1957) The initial value problem for transient water waves. Commun Pure Appl Math 10: 511-522.
18. Kara F (2000) Time domain hydrodynamics and hydroelastic analysis of floating bodies with forward speed.
19. Hess JL, Smith AM (1964) Calculation of non-lifting potential flow about arbitrary three-dimensional bodies. J Ship Res 8: 22-44.
20. Liapis SJ (1985) Time domain analysis of ship motions.
21. King BK, Beck RF (1987) Time domain analysis of wave exciting forces.
22. Newman JN (1990) The approximation of free surface green functions. Massachusetts Institute Technol. pp: 107-135.
23. Iversen LC (1982) Numerical method for computing the power absorbed by a phase-controlled point absorber. Appl Ocean Res 4: 173-180.
24. Greenhow M, White SP (1997) Optimal heave motion of some axisymmetric wave energy devices in sinusoidal waves. Appl Ocean Res 19: 141-159.
25. Eidsmoen H (1998) Tight-moored amplitude limited heaving buoy wave energy converter with phase control. Appl Ocean Res 20: 157-161.
26. Korde UA (2002) Latching control of deep water wave energy device using an active reference. Ocean Engineering 29: 1343-1355.
27. Babarit A, Duclos G, Clement AH (2004) Comparision of latching control strategies for a heaving wave energy device in random sea. Appl Ocean Res 26: 227-238.
28. Pierson WJ, Moskowitz L (1964) A proposed spectral form for fully developed wind seas based on the similarity theory of S.A. Kitaigorodskii. J Geophys Res 69: 5181-5190.
29. Ochi MK (2008) Ocean waves: The stochastic approach. Cambridge Ocean Technology Series 6.